Journal of Physics & Astronomy

Research | Vol 5 Iss 3

The Shape of the Universe: The Properties of Quadratically Expanding Space

Donald R Airey

Department of Astronomy, Wilder Road Bolton, USA

*Corresponding author: Donald R Airey, Department of Astronomy, Wilder Road Bolton, USA, Tel: +972 1-800-660-660; E-mail: don@airey.us

Received: October 03, 2016; **Accepted:** October 24, 2017; **Published:** October 31, 2017

Abstract

The relation between time and space is difficult to describe because we can't measure time directly and can only make inferences based on how the space between objects change from one moment to the next. The widely accepted FLRW metric describes an essentially linear relation between space and time. Here we show that space instead grows quadratically with time and that – as a result of a tiny but ubiquitous acceleration produced at every point in space – the least understood aspects of our universe – the accelerated expansion of space, the high velocity of stars and galaxies around a common center and the relation between mass and angular velocity in spiral galaxies – have a simple and geometric explanation.

Keywords: Cosmology; Large-scale structure of universe-cosmology; Theory-galaxies

Introduction

The known laws of motion and cosmology fail when applied to structures larger than our solar system. Stars move too quickly around galaxies to be bound by Newton's laws of motion. The Virial Theorem tells us that galaxy clusters have too much kinetic energy for the visible mass they contain. And the light from distant supernovae is too dim to be understood in terms of Hubble's law.

Most of our universe is missing when seen in the context of conventional theories. Only a small fraction – less than 5% – is occupied by things that we can measure directly. The rest is hidden. Placeholders for exotic forms of energy and matter are used in the ΛCDM model in an attempt to reconcile the observed universe with existing laws with the hope that they will someday be occupied by a discovery. This paper seeks to change some of those laws and, instead of placeholders, explain the missing universe in terms of a simple metric: the constant and quadratic expansion of space with time.

Experimental

Time and space

A metric of expansion of space was theorized by Georges Lemaître and confirmed by the observations of Edwin Hubble at a time when the instruments provided a limited view of the galactic neighborhood. The difference in age between the Lemaître metric (13.8 billion yrs) in a flat universe and the Hubble time (14.4 billion yrs) is not significant. The Lemaître metric has been – to the present epoch – an essentially a linear relationship between space and time.

Citation: Donald R Airey. The Shape of the Universe: The Properties of Quadratically Expanding Space. J Phys Astron. 2017;5(3):122

© 2017 Trade Science Inc.

The redshifts of distant novae now indicate that the expansion of our universe is accelerating [1]. Using existing laws, we can model an expansion that rapidly inflates, stops inflating, expands, decelerates and accelerates again and arrives through a fortunate coincidence at the nearly the same age provided by a linear expansion. Alternatively, out of a desire for simplicity, we can hypothesize a universe that has always been accelerating at the current rate. This requires a geometry that naturally accumulates space with time.

Our hypothetical universe is a hypersphere where the radius is the dimension of time and the surface at any given time consists of the three observable dimensions of space. All dimensions are mutually orthogonal and the total amount of space in a given dimension is equal to the square of the time. This is the basis of our metric for expansion.

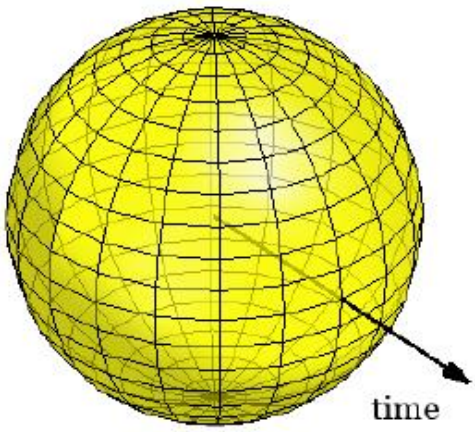

FIG. 1. **Simplified projection of the proposed universe ignoring orthogonality and one of the dimensions of space.**

A simplified schematic of the relation between time and space is shown in FIG. 1. This universe is a static shape that exists outside of time, but for an observer who experiences time sequentially, it's useful to describe space as a function of time. Applying this geometry, we can say that the circumference of each of the dimensions of space grows quadratically with time:

$Y=t^2$

Where, t is the age of the universe (s) and y is the circumference (s^2). Units of square seconds are not useful since distances are measured in units of space, so a way is needed to equate the surface of the hypersphere to something that can be observed directly:

$X=\varphi\ t2$

Where x is the circumference of the universe (km) and φ is the ratio of one kilometer to a square second ($km\ s^{-2}$)1. We can now describe how space changes with time.

$v=\varphi t^2 d/\mathrm{d}t=2\varphi t$

Where v is the rate by which the universe expands after time t, 2φ is the second derivative of expansion which we'll represent with $a0$ to highlight its function as a primordial acceleration constant. Substituting, we get:

$v=a_0 t$ (1)

Equation (1) provides a simple metric for describing the shape of the universe that can be tested against observed data. This metric is the analog of the FLRW metric [2] in ΛCDM.

The mechanics of expansion

We can now describe how space in our hypothetical universe grows given two ages. If $a0$ in a sample universe is $12 km\ s^{-2}$, then between the first and second minute the amount of space in each dimension would increase by $\int a0t12060\ dt$=2,700 km. How and, more importantly, where this growth occurs will profoundly affect the laws of motion in this universe.

One option is that space inflates like a balloon. The distances between points on the surface expand proportionally to the change in the balloon size. That is, each unit length grows pro-rata to the growth of the universe.

Another option and the one that best matches the observations is that every point in space is constantly pushing the existing space outward. To illustrate how this works, take the sample universe at 900 km in circumference after the first minute. An observer would see every object move away by 2,700 km in every direction after the second minute if this universe was flat and infinite.

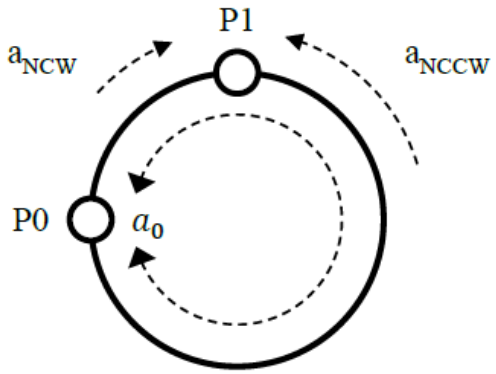

FIG. 2. **The object, P1, is pushed away from another object, P0, at a rate of ao in the clockwise direction. It is pushed in the counter clockwise direction by the same rate.**

But our hypothetical universe is closed. While space is expanding in front of an object, it is likewise expanding behind it. FIG. 2 illustrates that the clockwise acceleration of $a0$ meets a counter clockwise acceleration of $a0$ and so we have a

standoff. We know that an observer at P0 will look into the distance and see their own backside accelerate away at a rate of $a0$. But we don't yet have a clear description of the motion of P1 in relation to P0. We need to understand how the net acceleration in the clockwise direction, aNCW and the net acceleration in the counter clockwise direction, $aNCCW$, are related to the expansion.

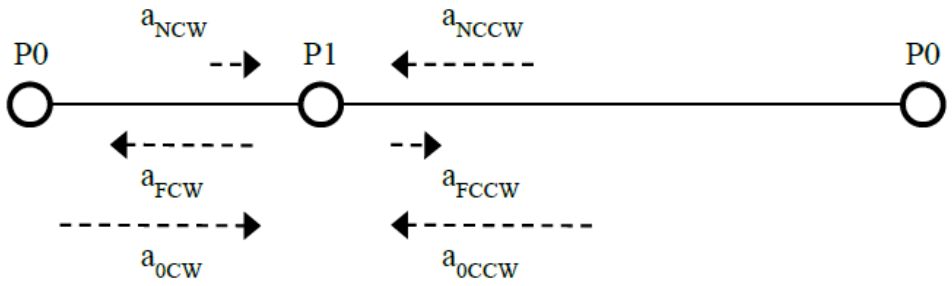

FIG. 3. **Some amount of the clockwise expansion of the universe, $a0CW$, originating from P0 passes through P1 and creates an acceleration back towards P0, $aFCW$. The net acceleration moves P1 in a clockwise direction at $aNCW$.**

FIG. 3 shows the components of the standoff schematically. The space originating from P0 in the clockwise direction – 2,700 km between the first and second minute in our example – will not only move P1 in a clockwise direction, but will also flow through P1 if proportions are to be maintained (that is, in quadratically expanding space an external force is not required to accelerate an object, but is required to change the ratios between objects. This is discussed in the next section.) The passage of space through an object is indistinguishable from an object moving through space. Therefore, the space originating from P0 creates an acceleration on P1 of $aFCW$ in the counter clockwise direction while simultaneously moving P1 in the clockwise direction for a net acceleration of $aNCW$. The same is true of the counter clockwise direction.

We're now in a position to make some quantitative statements about the movement of P1 in relation to P0. With no motion other than that provided by the quadratic expansion of a closed universe with time, the net accelerations, $aNCW$ and $aNCCW$, will remain constant and their sum will be $a0$. In order for $aNCW$ to remain constant in an expanding universe the acceleration at the start of an interval will be the same at the end of the interval, so the following conditions must be met:

$$\Delta x_0 + \int_{t_0}^{t_1} a_{NCW} t\, dt = \int_0^{t_1} a_{NCW}\, t\, dt$$

$$\Delta x_0 + \frac{1}{2} a_{NCW} (t_1^{\,2} - t_0^{\,2}) = \frac{1}{2} a_{NCW}\, t_1^{\,2}$$

$$a_{NCW} = \frac{2\Delta X_0}{t_0^{\,2}}$$

where $\Delta x0$ is the distance from P0 to P1 at $t0$ and $t0$ and $t1$ are two arbitrary ages. This formula sets up the conditions where the space accumulated during the interval – plus the original distance – is the same as the space accumulated since start of time. Solving for $aNCW$ we discover that the net acceleration is simply pro-rated by the ratio of its original distance to the size of the universe. That is, if $\Delta x0$ is ¼ of the circumference of the universe, then $aNCW$ will be ¼ of $a0$.

This means that even though P0 is the source of an outwardly directed acceleration caused by expanding space, in a closed universe the growth in luminous distances between P0 and P1 will be pro-rated to the growth of the whole universe, as in the FLRW metric expansion. However, an object travelling from P1 to P0 will find that the travel distance is longer than the luminous distance. As the object moves in the direction of P0 it must transverse the space that is constantly originating from P0. A photon travelling between two galaxies, for example, can travel several times the luminous distance between those two galaxies before it reaches its destination. This is a critical new feature of this geometry and will be used later in the derivation of the luminous distance formula in the discussion of the rate of expansion.

The Laws of Motion

The laws of motion will be different in a quadratically expanding hypersphere from those of a linearly expanding universe.

The first law of motion

Objects at rest tend to accelerate and objects in motion tend to accelerate. All objects accelerate with the expansion of the universe unless acted on by an unbalancing force.

Every point in the universe expands at a rate of $a0$ from every other point. Two objects can be at rest – or in uniform motion – with each other only when there is an unbalancing force keeping them in that position. In the absence of such an influence, the two bodies will drift apart. Some of the space created will be measurable by a ruler and the other portion as an expanding travel distance as an observer moves from the first object to the second.

The second law of motion

The change of momentum of a body is proportional to the unbalancing impulse impressed on the body plus the constant impulse impressed on the body by the expansion of the universe and happens along the straight line on which that unbalancing impulse is impressed.

For a constant mass system, this statement can be expressed in equation form:

$\boldsymbol{v}(\boldsymbol{t})=\boldsymbol{v0}+\boldsymbol{a0}t$

$$\sum_i F_i = \frac{dmv(t)}{dt} = \frac{d\,m(v_0 + v_0)}{dt},\ a_F = \frac{d_{v0}}{dt}$$

$$\sum_i F_i = m\left(a_F + a_0\right) \qquad (2)$$

Where $\boldsymbol{v0}$ is the initial velocity, $\boldsymbol{aF}$ is the acceleration due to the imbalance of forces and $\boldsymbol{a0}$ is the acceleration of expansion and is directed radially outward.

The third law of motion

To every action, there is always an opposite and unequal reaction: The mutual actions of two bodies upon each other are always unequal and differ by the impulse provided by the expansion of the universe.

The third law tells us that the amount of momentum in any action between two bodies in a quadratically expanding hypersphere is never completely conserved. When two forces oppose each other, the mutual force will be mitigated by the expansion of space which pulls all things apart.

$$\boldsymbol{aNCW}+\boldsymbol{aNCCW}=\boldsymbol{a0}$$
$$\boldsymbol{aNCW}=\boldsymbol{a0}-\boldsymbol{aNCCW}$$
$$m\boldsymbol{aNCW}=(\boldsymbol{a0}-\boldsymbol{aNCCW}) \qquad (3)$$

An observer will measure an object moving away at a net rate of $\boldsymbol{aNCW}$. That observer can turn around and look in the opposite direction and – with a powerful enough telescope – measure the same object moving away at a net rate of $\boldsymbol{aNCCW}$. The sum of the two net accelerations will equal, $\boldsymbol{a0}$. In fact, every object in the universe will be seen to be moving away from itself at $\boldsymbol{a0}$. The momentum of the object in the clockwise direction is equal to the momentum in the counter clockwise direction when the rate of expansion is included in the impulse.

If the rate of expansion is so tiny compared to the acceleration caused by other forces that – for all practical purposes – $\boldsymbol{a0}$ is zero, then those forces will appear to be equal and opposite and momentum will appear to be conserved.

The rate of expansion

Because of the uniform mass of the progenitor star, Type Ia Supernovae (SNe Ia) can be used as standard candles for measuring distances on a cosmological scale. The redshift is relatively easy to obtain and tells us how the universe has expanded since the light was emitted. The luminosity is less easy to measure accurately but provides a proxy for a distance measurement. The formula used to predict the luminous distance, dL, from the redshift, z, using the metric in equation (Error! Reference source not found.) is provided in Appendix A. Using equation (A3) and data from a large collection of SNe Ia, we can solve for the unknowns: the age of the universe and the acceleration constant.

Using the combined data from (Conley et al. 2011), (Rodney et al. 2012), (Jones et al. 2013) and (Rodney et al. 2015) and the parameters from (Rodney, et al. 2015) to normalize the sets, X2 curve fitting produces a near perfect match to the metric: the age of the universe is 210 Gyr and the acceleration constant, $a0$, is $3.88 \times 10^{-14}\ km\ s^{-2}$. The reduced X2 on the Quadratically Expanding Hypersphere (QEH) model of 0.72 makes it better fit to the SNe Ia data than the ΛCDM model with a reduced X2 of 1.47. The difference between the models becomes more obvious beyond z ≈ 1.5 as the QEH metric predicts increasingly brighter SNe than ΛCDM as shown in FIG. 4.

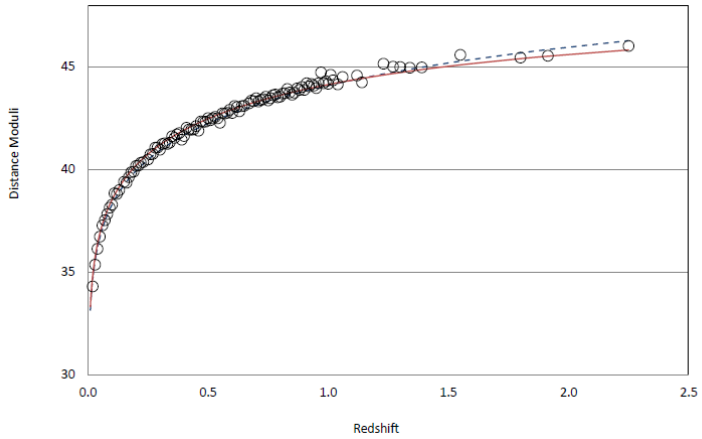

FIG. 4. **Observed distance moduli (circles) are plotted with the QEH predictions (solid line) and the ΛCDM predictions (dashed line). The formula used for the distance moduli is 5 log(dL)+25 (dL in units of Mpc).**

Spiral Galaxies

The effects of quadratic expansion would be measurable in low acceleration environments where aF ≈ a0. Spiral galaxies provide such a domain. We can calculate the mass of a body in quadratically expanding space using the velocity of an object in a circular orbit around that mass by applying the force of gravity and the acceleration of centripetal motion to equation (2) to get:

$$-\frac{GM(r)m}{r^2}\hat{r}=\left(-\frac{v^2}{r}+a_0\right)\hat{r} \qquad (4)$$

$$\frac{v^2}{r}=\frac{GM(r)}{r^2}+a_0 \qquad (5)$$

Where, for a given radius, r, M (r) is the enclosed mass, v is the angular velocity and G is the gravitational constant. Rearranging we can predict the velocity of an object circling a mass:

$$v = \sqrt{\frac{M(r)G}{r}} + a_0 r \qquad (6)$$

A mass model of a spiral galaxy is required to compare the prediction of equation (6) against the ΛCDM predictions. For QEH, the mass model consists of a bulge and a disk; a halo of Dark Matter is added for ΛCDM. The bulge in both models is assumed to have a de Vaucouleurs profile (de Vaucouleurs 1958) having a surface density of:

$$\sum b(R) = \sum_{be} \exp\left\{-k\left[\left(\frac{R}{a_b}\right)^{\frac{1}{4}} - 1\right]\right\} \qquad (7)$$

Where κ is 7.6695 and Σbe is the density at the scale radius, ab. Because an exact solution is computationally expensive and approximations are inaccurate, a deprojection table from [3] was used in the search for the best-fit parameters for the bulge mass.

The exponentially thin disk for both models is calculated from [4] as:

$$M_{disk}(R) = \int_0^R 2\pi r \sum o e^{\frac{r}{a_d}} dr$$

$$M_{disk}(R) = 2\pi \sum_o a_d \left(R_d - e^{\frac{-R}{a_d}}\left(R + a_d\right)\right) \qquad (8)$$

where Σ0 is the central surface density, ad is the scale length of the disk.

The NFW profile [5] is a good model for the Dark Matter halos in the outer regions of galaxies. Integrating the density profile, the mass can be expressed as:

$$M_{halo}(R) = \int_O^R 4\pi r^2 \frac{\rho_o}{\frac{r}{h}\left(1 + \left(\frac{r}{h}\right)^2\right)} dr$$

$$M_{halo}(R) = 2\pi\rho_o h^3\left(-In\left(h^2\right) + In\left(R^2 + h^2\right)\right) \qquad (9)$$

where $\rho 0$ is the Dark Matter characteristic density and h is the scale radius of the halo.

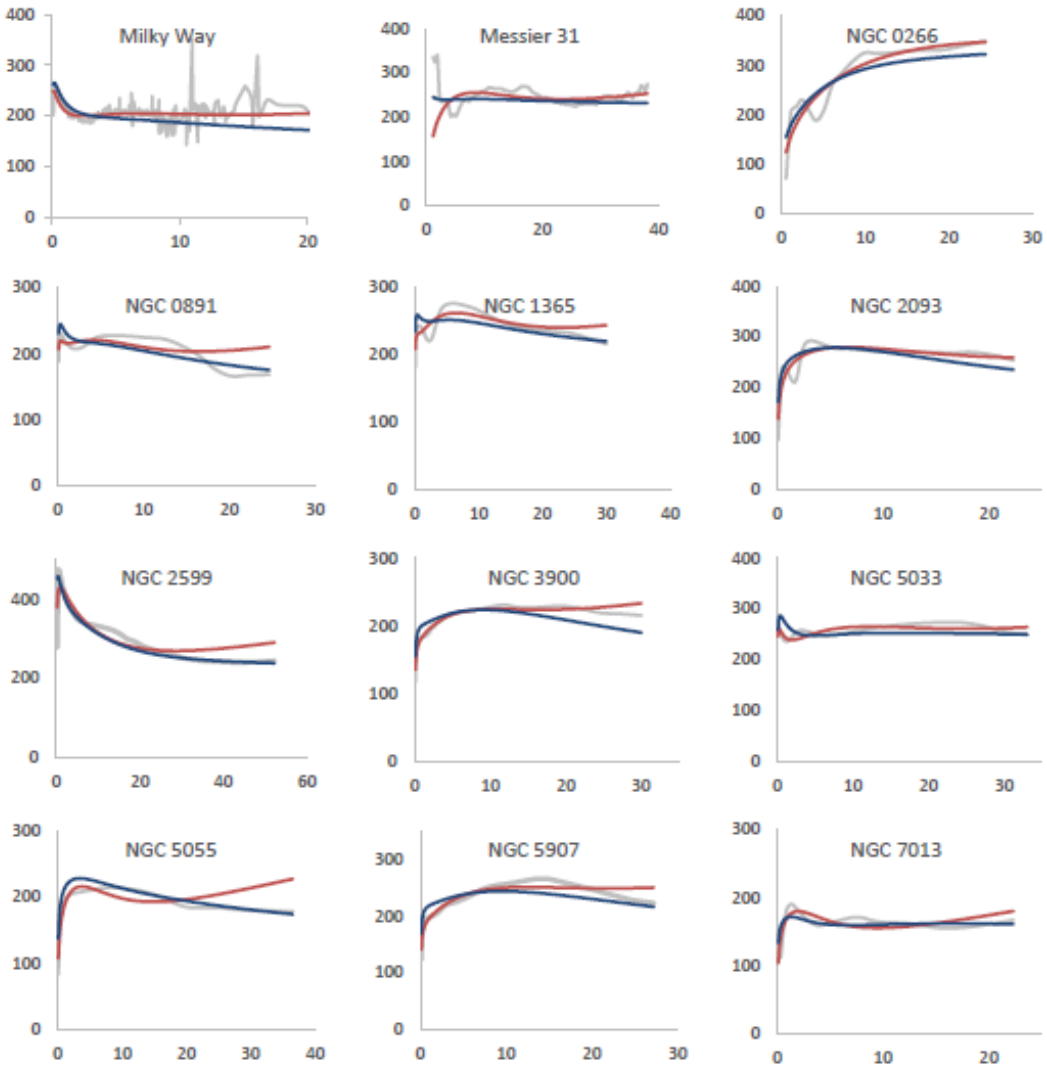

FIG. 5. **A sampling of the angular velocity predictions for QEH (red) and ΛCDM (blue) and the observed data (gray). All horizontal axes are radius in kpc. Vertical axes are angular velocity in km s^{-1}.**

Results and Discussion

Both models are fitted to the data from [5-13] for the Milky Way Galaxy, for Messier 31, The best-fit ΛCDM model parameters are taken from. A sample of the resulting rotational curves can be found in FIG. 5. Note that the effect of quadratically expanding space on the rotation curve is to flatten it in the domain where the acceleration due to gravity is

gradually offset by the acceleration of expansion. This is in contrast to the steady Keplerian drop off one would expect in flat, linear space.

TABLE 1. **The tabulated results of comparing the ΛCDM predictions against the QEH predictions.**

				ΛCDM						**QEH**		
Name	**ab (kpc)**	**Mb (10^{10} $M_\odot$)**	**ad (kpc)**	**Md (10^{10} $M_\odot$)**	***h* (kpc)**	**Mh (10^{10} $M_\odot$)**	X^2	**ab (kpc)**	**Mb (10^{10} $M_\odot$)**	**ad (kpc)**	**Md (10^{10} $M_\odot$)**	X^2
Milky Way	0.52	1.65	3.19	3.41	12.50	5.02	10.92	0.41	1.13	3.59	7.51	4.03
NGC 0224	1.30	3.36	4.30	7.70	30.50	27.90	27.85	1.00	0.00	3.78	16.64	19.23
NGC 0253	0.93	1.60	1.90	1.90	7.90	3.50	326.48	0.64	0.86	2.46	5.93	155.70
NGC 0266	2.89	2.12	6.60	25.10	87.10	239.30	1,545.58	10.00	5.46	11.96	79.72	904.21
NGC 0342	0.64	0.52	1.60	1.60	12.00	7.90	91.78	1.30	0.83	2.85	5.83	13.92
NGC 0598	7.66	0.22	6.10	0.50	8.50	2.40	29.69	1.00	0.00	1.92	0.66	26.74
NGC 0660	0.57	0.94	0.60	0.20	9.20	3.80	25.34	0.39	0.59	1.25	1.53	135.74
NGC 0891	0.71	1.84	3.10	3.10	6.40	3.10	313.24	0.64	1.29	2.82	7.11	276.07
NGC 1365	0.90	2.51	3.30	6.60	14.40	10.40	439.67	0.77	1.60	3.68	14.47	195.60
NGC 1642	3.06	2.78	3.00	6.00	88.90	83.10	260.34	1.04	0.06	2.34	7.87	172.40
NGC 2403	0.14	0.02	0.20	0.00	7.60	2.90	42.32	0.60	0.08	2.20	1.21	56.67
NGC 2543	0.99	0.15	3.80	4.00	20.60	14.10	337.91	3.69	0.38	6.67	13.93	180.47
NGC 2599	1.08	10.03	3.50	12.50	50.20	43.80	1,314.98	2.96	24.62	3.72	2.24	975.53
NGC 2599	1.08	10.03	3.50	12.50	50.20	43.80	1,314.98	2.96	24.62	3.72	2.24	975.53
NGC 2649	1.56	0.16	3.10	3.10	19.70	11.70	124.38	9.14	0.21	4.07	7.23	9.39
NGC 2654	1.07	1.45	2.80	5.70	52.90	38.20	346.30	0.45	0.37	2.49	7.39	185.05
NGC 2903	2.50	5.24	3.80	8.00	7.60	5.00	670.73	5.20	10.11	4.38	13.41	366.80
NGC 2985	0.56	0.39	1.10	1.10	9.70	4.20	25.14	0.67	0.49	1.51	2.18	636.57
NGC 3079	0.69	2.63	3.80	4.40	16.20	9.50	477.67	0.74	2.25	4.36	10.03	233.76
NGC 3198	6.21	0.50	3.10	1.60	13.40	6.20	165.51	1.00	0.00	3.42	3.85	282.15
NGC 3521	0.72	1.52	1.60	3.50	22.60	14.00	406.18	0.07	0.18	1.58	6.72	73.55
NGC 3628	0.84	1.52	3.60	3.60	8.50	4.80	170.05	1.32	2.00	5.07	11.04	34.08
NGC 3900	1.66	2.44	6.30	11.90	7.70	2.80	252.55	1.63	1.77	4.49	11.34	42.47
NGC 3982	0.55	0.09	1.20	1.20	23.60	13.80	102.88	3.90	0.40	1.67	2.37	8.92
NGC 4258	0.47	1.19	0.80	0.90	19.40	16.10	209.35	1.76	4.18	8.24	5.05	111.67
NGC 4303	0.33	0.15	2.10	1.10	11.90	4.50	318.52	0.26	0.11	2.16	2.04	429.51
NGC 4321	1.32	2.76	7.60	16.80	7.10	4.20	347.82	1.73	2.96	6.80	23.93	91.52
NGC 4527	0.41	0.94	2.60	1.70	12.20	7.40	502.75	0.45	0.95	4.29	7.66	423.65
NGC 4565	3.05	6.40	4.00	4.60	19.20	16.30	551.64	10.69	26.75	5.48	1.62	268.58
NGC 4569	1.39	0.66	12.00	39.70	9.80	3.50	892.04	2.52	1.01	20.00	89.42	462.48
NGC 4736	0.82	1.09	0.90	0.80	7.30	2.30	212.82	2.00	2.82	1.49	0.78	138.75
NGC 4945	0.36	0.69	0.30	0.30	9.00	5.60	92.88	11.10	9.95	0.15	0.48	95.20
NGC 5033	1.04	3.76	5.70	11.40	38.90	41.20	421.40	0.69	2.03	5.59	21.56	90.44

NGC 5055	2.96	4.15	1.80	1.70	7.70	4.20	385.20	2.63	1.87	2.12	5.15	277.36
NGC 5236	0.19	0.47	3.00	1.80	8.10	4.40	249.21	0.16	0.40	2.88	4.83	618.65
NGC 5457	2.76	2.90	2.40	2.20	8.10	4.60	426.31	14.14	25.91	1.00	0.00	210.65
NGC 5907	1.60	2.76	6.90	13.80	6.70	3.40	402.47	1.75	2.13	5.30	17.68	96.58
NGC 6946	0.36	0.92	3.80	4.20	9.40	5.60	199.42	0.36	0.81	4.47	11.20	112.59
NGC 7013	0.82	0.64	0.80	0.80	11.80	5.70	229.69	2.23	1.34	1.18	1.74	170.75
UGC 03993	4.35	16.59	4.80	7.50	135.10	214.90	245.45	1.78	4.36	3.70	16.39	124.69
Average							362.74					242.19

The results of comparing the best-fit parameters of the two models against the observed data are collected in TABLE 1. Out of the 43 galaxies selected for the [10] study, three galaxies (NGC 5533, UGC 02916, UGC 11852) were rejected because the velocities of gas in the outer disks were incompatible with regular motion. Except for the Milky Way and Messier 31, the errors for the observed data were assumed to be unity (1 km s^{-1}) and the modified X2 method described in [10] was used (which is, essentially, a least-squares method). Of the 40 galaxies, the observed data in 33 were significantly better matches to the QEH predictions than the ΛCDM predictions. In aggregate, the QEH model is also a better match with a average modified X2 of 237.59 compared to ΛCDM with a average modified X2 of 364.73. Note that ΛCDM requires an undiscovered particle, two additional parameters and still doesn't fit the data as well as QEH.

Missing mass

Quadratically expanding space would have the appearance of missing mass to an observer who believed that the expansion of space with time had no impact on the laws of motion. That is, the application of Newton's second law of motion to events in the QEH universe will result in more mass than actually exists. This would be especially obvious in low acceleration domains such as galaxy clusters. Here we examine the gas pressure and the gravity in these clusters to test the theory that the missing mass of Newtonian physics is the simply the local effects of an expanding universe.

Galaxy clusters are believed to be in a state of hydrostatic equilibrium where the motion caused by the pressure of the intracluster medium (ICM) as it heats is offset by the force of gravity. Using the formulas from [14] for the acceleration resulting from the expanding gas and equation (2), the sum of forces in the QEH universe can be written as:

$$-\frac{GM_{QEH}(r)m}{r^2}\hat{r} = m\left(\frac{1}{\rho_g}\frac{dp}{dr} + a_o\right)\hat{r}$$

$$M_{QEH}(r) = -\left(\frac{1}{\rho_g}\frac{dp}{dr} + a_o\right)\frac{r^2}{G} \qquad (10)$$

where $MQEH(r)$ is the mass enclosed inside radius, r, in the QEH universe, ρg is the gas density and P is the pressure of the gas. For the same system, Newton would measure a larger mass:

$$M_N(r) = -\left(\frac{1}{\rho_g}\frac{dp}{dr}\right)\frac{r^2}{G} \qquad (11)$$

where $MN(r)$ is the mass enclosed inside radius, r, in linearly expanding space. Therefore, an observer using Newton's second law of motion in a universe where every point accelerates outward at a rate of $a0$, would be unable to account for the following mass:

$$\Delta M(r) = M_N(r) - M_{QEH}(r)$$

$$\Delta M(r) = -\left(\frac{1}{\rho_g}\frac{dp}{dr}\right)\frac{r^2}{G} + \left(\frac{1}{\rho_g}\frac{dp}{dr} + a_0\right)\frac{r^2}{G}$$

$$\Delta M(r) = \frac{a_0 r^2}{G} \qquad (12)$$

We examined the stellar, gas and Dark Matter components in [15-18] From these studies, we found the equivalent Hubble parameter, h0, in the QEH geometry using the red-shift of each galaxy. Once we corrected for the distance, it was a straight-forward matter to calculate the Dark Matter mass as the difference of the total mass and the gas fraction. We then compared the Dark Matter mass against the missing mass of equation (12) for 219 galaxy clusters and the results are displayed in FIG. 6. A coefficient of determination, R2, of 0.88 strongly suggest that Dark Matter is the error one would calculate using Newtonian physics in quadratically expanding space.

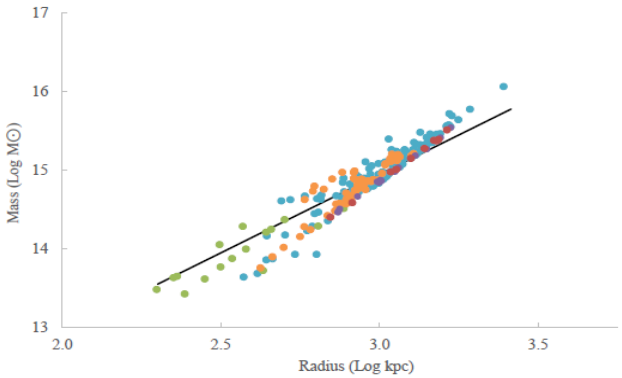

FIG. 6. **The Dark Matter mass, corrected for distance, of Vikhlinin (red), Gastaldello (green), Gonzalez (purple) and Eckert (aqua) overlaid with the function $\frac{a_0 r^2}{G}$ (black).**

The fundamental plane

The second law of motion in quadratically expanding space defines a plane of possible masses given the two free parameters: the angular velocity and the radius of orbiting objects. Formula (5) can be rearranged to predict the mass given the velocity and radius.

$$M\left(r\right)=\frac{\left(v^2-a_0 r\right)r}{G} \qquad (13)$$

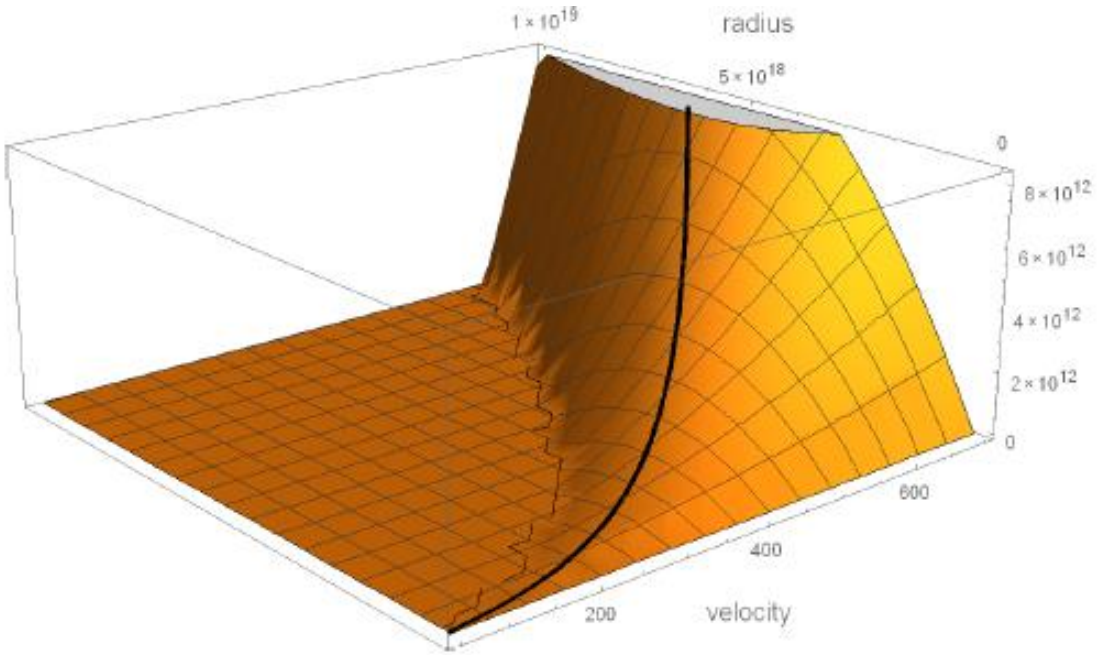

FIG. 7. **The fundamental plane of Mass. Radius is in km, velocity in km s^{-1} and the vertical axis is in M⊙. Solid line is the maximum mass allowed by the QEH second law of motion.**

FIG. 7 shows the plot of mass as a function of radius and angular velocity. The radius where the maximum mass will be found is:

$$M\left(r\right)=\frac{\left(v^2-a_0 r\right)r}{G}\frac{d}{dr}=0$$

$$\frac{v^2-2a_0 r}{G}=0$$

$$r=\frac{v^2}{2a_0} \qquad (14)$$

Substituting the equation (14) back into equation (13) yields the formula for the maximum mass given the velocity:

$$M_{MAX} = \frac{\left(v^2 - a_0 \frac{v^2}{2a_0}\right)\frac{v^2}{2a_0}}{G}$$

$$M_{MAX} = \frac{v^4}{4a_0 G}$$

$$M_{MAX} = 48.58v^4 \qquad (15)$$

Here the velocity is in units of km s^{-1} and the maximum mass, $MMAX$, is in units of M⊙. A study of the relation between velocity and mass was conducted in [19] with the assumption that luminosity is an imperfect proxy for mass. Gas rich galaxies are a better proxy as they are not as effected by the vagaries of the stellar mass-to-light ratios. Those results are displayed in FIG. 6 and overlaid with equation (15). The reduced X2 of 0.65 demonstrates that the QEH second law of motion accurately predicts the Baryonic Tully-Fisher Relationship (BTFR).

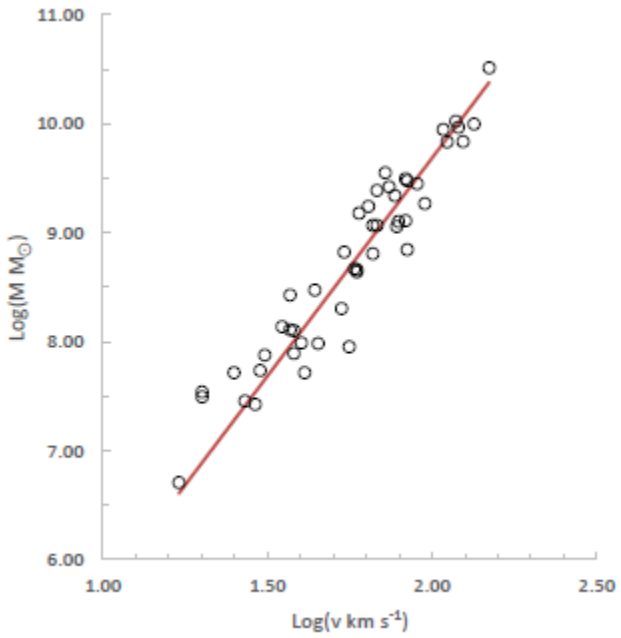

FIG. 8. **Relation between angular velocity and mass. Circles are the combined gas and stellar mass of the gas-rich galaxies and the solid line is the maximum mass allowed by the QEH second law of motion.**

Conclusion

A complete comparison of cosmological models would include an analysis of Cosmic Microwave Background (CMB) radiation and Baryonic Acoustic Oscillations (BAO) which provide geometric constraints on the early universe. An exhaustive analysis is beyond the scope of this document but a back-of-the-envelope calculation using the QEH metrics show the luminous distance to the Surface of Last Scattering, d_{sls}, is 69.72 Gpc using equation (A3). The age of the universe at decoupling (z=1090) was 6.38 Gyr using equation (A2) and so – assuming the speed of sound in plasma is $\frac{C}{\sqrt{3}}$ – the sound horizon, rs, at decoupling is 1.13 Gpc.

Using $l = \frac{\pi d_{sls}}{r_s}$ the first acoustic peak at 194 *l* in the QEF model is consistent with the observed value of 220 *l* from the 2013 Plank Study [20] The current circumference of the universe of 27.70 Gpc tells us that large scale correlations of baryonic matter (that is, the imprint of the sound horizon on the present-day universe) should be seen at 147 Mpc which compares to the correlation of matter at 142 Mpc measured by [21] using *H0=67.70*. Based on these rough calculations, the QEF geometry is compatible with CMB and BAO observations.

No theory of cosmology is complete without an explanation of the observed relationship between the mass and the spectral line width of a spiral galaxy, the BTFR. The Newtonian second law of motion assumes that the expansion of the universe has no effect on the laws of motion and without a direct relation between orbital velocity and mass – independent of the radius – a satisfactory explanation of the BTFR is impossible. However, in QEH, this relation is simply the maximum mass allowed at a given angular velocity. The BTFR is incontrovertible evidence written in the night sky of the QEH second law of motion.

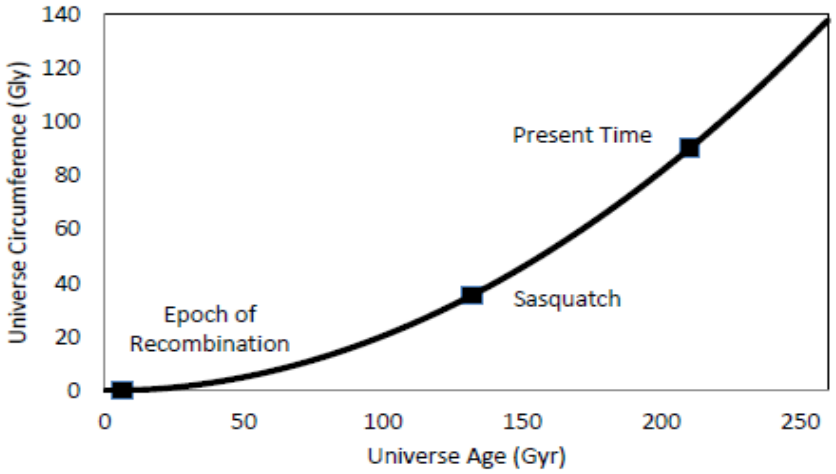

FIG. 9. **The relation of space (Gly) to time (Gyr).**

The QEH model is a better fit to the observed data than ΛCDM and requires less assumptions. The universe can be modelled as a four-dimensional hypersphere that expands naturally at a constant rate of $3.88 \times 10^{-14}\ km\ s^{-2}$. The age of the QEH universe is 210 Gyr and it has acircumference of 90.35 Gly. FIG. 9 shows that a photon from Sasquatch (z of 1.39) has been travelling for 74.3 Gyr and has an effective velocity of 0.29 c as it fights for progress against quadratically expanding space. The age of this universe is more than an order of magnitude older than that predicted by the ΛCDM model which requires a complex series of 'phases' where the entire universe jerks back and forth by a coalition of changing forces. In contrast, the QEH metric employing a constant acceleration is a kinematically trivial solution to the SNe Ia data and rotational curve data with no requirement for energies or particles or fields that have yet to be discovered [22-26].

Appendix A

Here is provided the derivation of the formulas used to predict the luminous distance moduli to a SNe Ia given the redshift. The distance travelled by a photon in a quadratically expanding universe, where the light is travelling towards the destination at the velocity of light, c and the universe is effectively travelling away at a rate of expansion, is described by the following integration:

$$\Delta x = \int_{t0}^{t1} (c - a_0 t)\, dt$$

$$\Delta x = \int_{t0}^{t1} c\, dt - \int_{t0}^{t1} a_0 t\, dt$$

$$\Delta x = c t_1 - c t_0 - \frac{a_0}{2} {t_1}^2 + \frac{a_0}{2} {t_0}^2$$

$$\Delta t = t_1 - t_0$$

$$\Delta x = c\Delta t = a_0 t_1 \Delta t + \frac{a_0}{2} \Delta t^2 \qquad \text{(A1)}$$

Where Δx is light travel distance, Δt is the light travel time, $t1$ is the age of the universe at the time of the observation and $t0$ is the age of the universe at the time the photon was emitted.

The redshift is a direct indication of how a single wavelength of light has expanded from the time it was emitted to the time it was observed. It is also a direct measurement of how the size of the entire universe has grown during that time. From the redshift, we can calculate the light travel time:

$$Z = \frac{\lambda_{OBSERVED} - \lambda_{EMIT}}{\lambda_{EMIT}}$$

$$Z = \frac{\varphi t_1^{\,2} - \varphi t_0^{\,2}}{\varphi t_0^{\,2}}$$

$$Z + 1 = \frac{t_1^{\,2}}{t_0^{\,2}}$$

$$Z + 1 = \frac{t_1^{\,2}}{\left(t_1 - \Delta_t\right)^2}$$

$$\Delta t = \frac{\left(1+z\right)t_1 \pm \sqrt{\left(1+z\right)}t_1^{\,2}}{1+z} \qquad \text{(A2)}$$

where z is the redshift, $\varphi t0^2$ is the size of the universe when the photon was emitted and $\varphi t12$ is the size of the universe when it is observed.

Now, to calculate the luminous distance in terms of the light travel distance and light travel time, we make use of the relationship between the observed distance, dL and the distance between the objects when the light was emitted, $d0$, which is:

$$\frac{d_L}{\varphi t_1^{\,2}} = \frac{d_0}{\varphi t_0^{\,2}}$$

This simply states that the space between the observer and emitter as a proportion of the entire universe doesn't change with time.

$$d_L = \frac{d_0 t_1^{\,2}}{\varphi t_0^{\,2}}$$

$$d_L = \frac{d_0 t_1^{\,2}}{\varphi\left(t_1 - \Delta t\right)^2}$$

$$d_L = \left(t_1^{\,2} - 2t_1\Delta t + \Delta t^2\right) = d_0 t_1^{\,2}$$

$$\frac{d_L = \left(t_1^{\,2} - 2t_1\Delta t + \Delta t^2\right)}{t_1^{\,2}} = d_0$$

$$d_L - d_0 = d_L \frac{2\Delta t}{t_1} - d_L \frac{2t^2}{t_1^{\,2}}$$

This represents the total change in distance that has occurred between the observer and the emitter while the light was travelling.

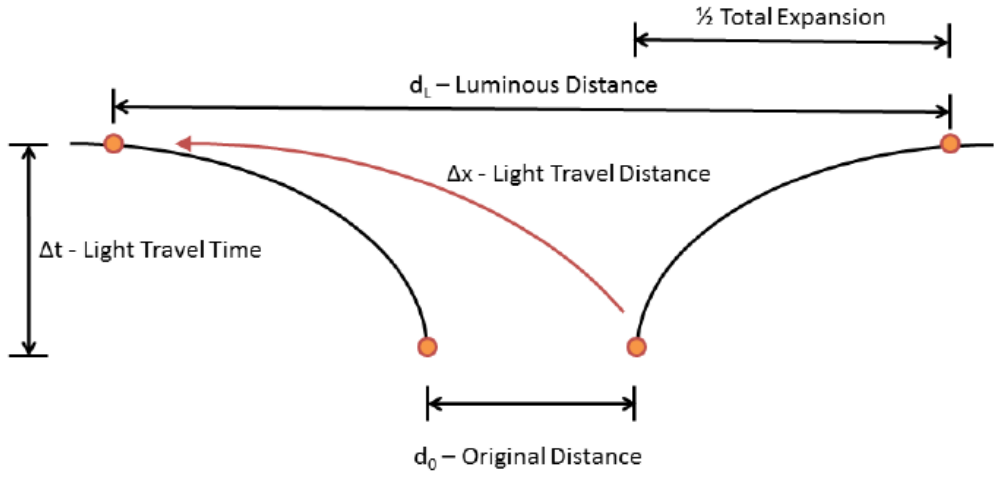

FIG. 10. **Total light travel distance, Δ*x*, is the observed distance to the object, *d*L, less one half of the expansion that occurred while the light was travelling.**

The next step exploits the fact that the light travel distance, Δx, is the difference between the luminous distance, dL and half of the total change in distance described in the previous formula as depicted in FIG. 9.

$$\Delta x = d_L - \frac{1}{2}\left(d_L \frac{2\Delta t}{t_1} - d_L \frac{\Delta t^2}{t_1^{\,2}} \right)$$

$$\Delta x = d_L - d_L \frac{\Delta t}{t_1} + d_L \frac{\Delta t^2}{2t_1^{\,2}}$$

$$d_L = \frac{\Delta x}{1 - \frac{\Delta t}{t_1} + \frac{\Delta t^2}{2t_1^{\,2}}}$$

Substituting equations (A1) and (A2) into this formula gives us the relation between the red-shift and the luminous distance:

$$d_L = \frac{a_0 t_1^{\,2} z + 2c\left(-t_1 (1+z) + \sqrt{t_1^{\,2}(1+z)} \right)}{2+z} \qquad \text{(A3)}$$

Acknowledgments

This research has made use of the NASA/IPAC Extragalactic Database (NED) which is operated by the Jet Propulsion Laboratory, California Institute of Technology, under contract with the National Aeronautics and Space Administration.

REFERENCES

1. Riess AG, Louis GS, John T, et al. Type Ia Supernova discoveries at z>1 from the Hubble Space Telescope: Evidence for past deceleration and constraints on dark energy evolution. The Astronomical Journal. 1998;116:1009.
2. Ellis GFR, Van Elst H. Dynamics of Pressure-Free Matter in General Relativity. NATO Sci SerC. 1999;541:1.
3. Young P. A protein kinase involved in the regulation of inflammatory cytokine biosynthesis. The Astronomical Journal. 1976;81:807.
4. Freeman KC. The radial velocity experiment (RAVE): First data release. The Astrophysical Journal.1970; 160:811.
5. Navarro JF. The structure of cold dark matter halos (Cambridge University Press) In Symposium-International Astronomical Union. 1996;255.
6. Sofue Y, Honma M, Omodaka T. Unified Rotation Curve of the Galaxy-Decomposition into de Vaucouleurs Bulge, Disk, Dark Halo and the 9-kpc Rotation Dip. Publications of the Astronomical Society of Japan. 2009;61:227.
7. Chemin L, Carignan C, Foster T. H I kinematics and dynamics of Messier. The Astrophysical Journal. 2009; 705:1395.
8. Sofue Y, Tutui Y, Honma M, et al. Central rotation curves of spiral Galaxies. The Astrophysical Journal. 1999; 523:136.
9. Sofue Y, Koda J, Nakanishi H, et al. The Virgo high-resolution CO survey: II. Rotation curves and dynamical mass distributions. Astronomical Society of Japan. 2003;55:59.
10. Sofue Y. Rotation curves of spiral galaxies. Astronomical Society of Japan. 2016; 68.
11. Garrido O, Marcelin M, Amram P, et al. A Virgo high-resolution Hα kinematical survey-II. The Atlas. Astronomical Society. 2005;362:127.
12. Noordermeer E, Van Der Hulst J, Sancisi R, et al. The Westerbork HI survey of spiral and irregular galaxies-III HI observations of early-type disk galaxies. Astronomical Society. 2007;376:1513.
13. Martinsson TP, Verheijen MA, Westfall KB, et al. Galaxy disks are submaximal. Astronomy & Astrophysics. 2013; 557:131.
14. Sarazin CL. X-ray emission from clusters of galaxies. Reviews of Modern Physics. 1988;58.
15. Vikhlinin A, Kravtsov A, Forman W, et al. Chandra sample of nearby relaxed Galaxy clusters: Mass, gas fraction and mass-temperature relation. The Astrophysical Journal. 2006;640:691.
16. Gastaldello F, Buote DA, Humphrey PJ, et al. A Chandra view of dark matter in early-type galaxies. The Astrophysical Journal. 2007;669:158.

17. Gonzalez AH, Sivanandam S, Zabludoff AI, et al. Galaxy cluster Baryon fractions revisited. The Astrophysical Journal. 2013;778:14.
18. Eckert D. Mechanisms of viral membrane fusion and its inhibition. Astronomy & Astrophysics. 2016;592:12.
19. McGaugh SS. Modified Newtonian dynamics as an alternative to dark matter. The Astronomical Journal. 2012; 143:40.
20. Ade PAR, Aghanim N, Arnaud M, et al. Planck 2015 results-XIII. Cosmological parameters. Astron Astrophys. 2014;571:16.
21. Seo HJ, Eisenstein DJ. Detection of the baryon acoustic peak in the large-scale correlation function of SDSS luminous red galaxies. The Astrophysical Journal. 2005;633:575.
22. Conley A, Astier P, Blanc G, et al. New constraints on ωm, ωΛ and w from an independent set of 11 high-redshift supernovae observed with the hubble space telescope. Astrophys J Suppl. 2011; 192:1.
23. Vaucouleurs DG. Statistical properties of bright galaxies in the sloan digital sky survey photometric system. The Astrophysical Journal. 1958;128:465.
24. Jones DO, Samantha L, Jeffrey M, et al. A 2.4% determination of the local value of the Hubble constant. Astrophys J. 2013;768:166.
25. Rodney SA, Robaina AR, Rix HW, et al. CANDELS: The cosmic assembly near-infrared deep extragalactic legacy survey. The Astrophysical Journal. 2012;746:5.
26. Rodney SA, Dan C, Wei Z, et al. Clash: Three Strongly Lensed Images of a Candidate Z ≈ 11 Galaxy. Astron J. 2015;150:156.